Research Square

Preprints are preliminary reports that have not undergone peer review.
They should not be considered conclusive, used to inform clinical practice,
or referenced by the media as validated information.

SO3H supported on NiFe2O4@SiO2-AP nanoparticles as an efficient and heterogeneous reusable catalyst for synthesis of pyridine derivatives

Mohammad abushuhel

abushuheilmohammad@gmail.com

Hourani Center for Applied Scientific Research, Al-Ahliyya Amman University

G. Padma Priya

JAIN (Deemed to be University)

Baraa Mohammed Yaseen

Alnoor University

Subhashree Ray

IMS and SUM Hospital, Siksha 'O' Anusandhan (Deemed to be University)

Y. Sasikumar

Sathyabama Institute of Science and Technology

Renu Sharma

University Institute of Sciences, Chandigarh University

Abhayveer Singh

Chitkara University Institute of Engineering and Technology, Chitkara University

Rasul Usmanov

Urgench State University Urgench

Khushnud Azizjanov

Ma'mun University

Research Article

Keywords: NiFe2O4, Nanoparticles, SO3H, Pyridine

Posted Date: March 18th, 2026

DOI: https://doi.org/10.21203/rs.3.rs-8986183/v1

License: This work is licensed under a Creative Commons Attribution 4.0 International License. Read Full License

Additional Declarations: No competing interests reported.

SO_3H supported on $NiFe_2O_4$@SiO_2-AP nanoparticles as an efficient and heterogeneous reusable catalyst for synthesis of pyridine derivatives

Mohammad abushuhel[1*], G. Padma Priya[2], Baraa Mohammed Yaseen[3], Subhashree Ray[4], Y. Sasikumar[5], Renu Sharma[6], Abhayveer Singh[7], Rasul Usmanov[8], Khushnud Azizjanov[9]

[1]Faculty of Allied Medical Sciences, Hourani Center for Applied Scientific Research, Al-Ahliyya Amman University, Amman, Jordan. Email: abushuheilmohammad@gmail.com
[2]Department of Chemistry and Biochemistry, School of Sciences, JAIN (Deemed to be University), Bangalore, Karnataka, India, Email: g.padmapriya@jainuniversity.ac.in
[3]Department of Medical Laboratory Technics, College of Health and Medical Technology, Alnoor University, Mosul, Iraq, Email: baraa.mohammed@alnoor.edu.iq
[4]Department of Biochemistry, IMS and SUM Hospital, Siksha 'O' Anusandhan (Deemed to be University), Bhubaneswar, Odisha-751003, India, Email: subhashreeray@soa.ac.in
[5]Department of chemistry, Sathyabama Institute of Science and Technology, Chennai, Tamil Nadu, India, Email: sasikumar.chemistry@sathyabama.ac.in
[6]Department of Chemistry, University Institute of Sciences, Chandigarh University, Mohali, Punjab, India, Email: drrenusharma01@outlook.com
[7]Centre for Research Impact & Outcome, Chitkara University Institute of Engineering and Technology, Chitkara University, Rajpura, 140401, Punjab, India, Email: abhayveer_singh@outlook.com
[8]Department of Chemistry Urgench State University Urgench, Uzbekistan, Email: rasul.u@urdu.uz
[9]Department of Natural Sciences, Ma'mun University, Khiva, Uzbekistan, Email: khushnud1977@gmail.com

Abstract

In the current study, the $NiFe_2O_4$@SiO_2-AP-SO_3H heterogeneous nanocatalyst demonstrated high efficiency in catalyzing the synthesis of pyridine derivatives. This prepared nanocatalyst proved to be a robust and environmentally friendly nano-reactor for the production of pyridine derivatives. The eco-conscious heterogeneous catalyst was thoroughly characterized using various techniques, including Fourier transform infrared spectroscopy, transmission and scanning electron microscopies, energy-dispersive X-ray spectroscopy, inductively coupled plasma optical emission spectroscopy, X-ray diffraction, and thermal gravimetric analysis. Key advantages of this method include the use of a green medium, straightforward separation and workup procedures, exceptional reusability of the nanocatalyst, and significantly reduced reaction time.

Keywords: $NiFe_2O_4$, Nanoparticles, SO_3H, Pyridine.

1. Introduction

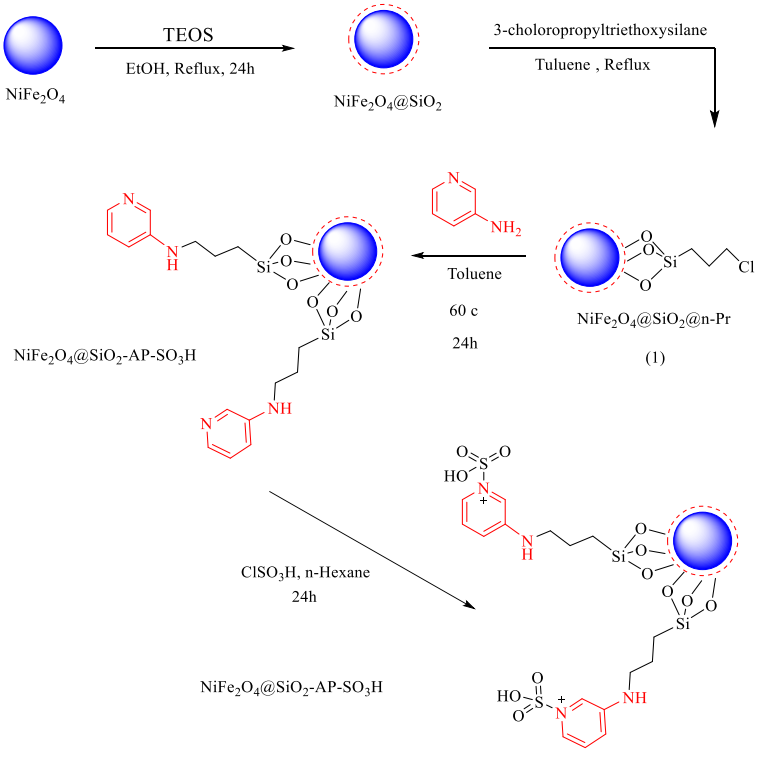
Developing efficient and innovative nanomaterials for catalyst support is a significant challenge in modern organic synthesis research[1–3]. Recently, nanostructured materials, particularly magnetic nanoparticles, have gained recognition as exceptional supports due to their large surface area, straightforward preparation and functionalization, and easy recovery with a magnetic field[4–6]. This leads to reduced operational costs and enhanced product purity[5,7]. One of the most notable advantages of magnetic nanoparticles is their effortless separation from the reaction mixture using a simple bar magnet[8–10]. Among heterogeneous catalysts, $NiFe_2O_4$ has become highly favored because of its facile synthesis and ability to be modified with a magnet[11]. These $NiFe_2O_4$ nanoparticles can support a variety of catalysts, facilitating easy separation even after multiple reaction cycles[9,12–14].

The synthesis of pyridine has garnered significant attention due to its extensive applications in the fields of biology and pharmaceuticals[15–19]. These compounds are highly valued as organic materials, especially for their function as photoactive agents and cosmetic colorants[20,21]. In recent years, their remarkable versatility and efficiency have led to the exploration of different catalysts aimed at enhancing the synthesis process[22–27]. This study emphasizes the design and structural analysis of an innovative, environmentally friendly catalyst tailored to stabilize SO_3H ligands. The research seeks to assess its effectiveness and sustainability as a catalyst for the efficient production of pyridine derivatives.

2. EXPERIMENTAL

2.1. Preparation of $NiFe_2O_4@SiO_2$-AP-SO_3H

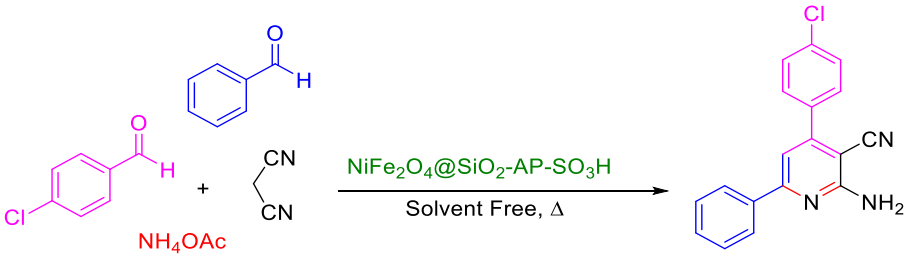
For the synthesis of $NiFe_2O_4@SiO_2$-AP-SO_3H nanocatalyst, first $NiFe_2O_4@SiO_2$@n-Pr-Cl were synthesized by co-precipitation method[28,29]. To synthesize the $NiFe_2O_4@SiO_2$-AP-SO_3H complex, 2 g of the prepared $NiFe_2O_4@SiO_2$@n-Pr-Cl was dispersed in 35 mL toluene by sonication for 55 minutes. Next, 5 mmol of AP (3-aminopyridine) was introduced into the flask and agitated at 60˚C for 24 hours. Once the reaction concluded, the resulting $NiFe_2O_4@SiO_2$-AP compound was isolated using magnetic decantation, cleansed with hexane and EtOAc, and subsequently dried at 75 °C in an oven for 24 hours. To prepare the $NiFe_2O_4@SiO_2$-AP-SO_3H catalyst, a combination of 2.0 g $NiFe_2O_4@SiO_2$-AP was dispersed in 75 ml of n-hexane in a round-bottomed flask. Next, 0.4 g of chlorosulfonic acid was slowly introduced into the reaction vessel and stirred at 25 °C for 24 hours. After the reaction was complete, the resulting $NiFe_2O_4@SiO_2$-AP-SO_3H catalyst was isolated, washed with H_2O and ethanol, and dried under vacuum at 55 ºC (Scheme 1).



Scheme 1 Synthesis of $NiFe_2O_4@SiO_2$-AP-SO_3H

2.3. General procedure for the synthesis of pyridine derivatives

A reaction mixture was created using aryl aldehyde (1 mmol), malononitrile (1 mmol), acetophenone (1 mmol), ammonium acetate (1 mmol), and the $NiFe_2O_4$@SiO_2-AP-SO_3H catalyst (20 mg). The mixture was stirred at 80 ˚C for a suitable period while monitoring the reaction progress with thin-layer chromatography (TLC), utilizing a solvent system of hexane and ethyl acetate in a 7:3 ratio. After completion, the mixture was diluted with hot ethanol, allowing for the separation of the catalyst, which was meticulously washed with hot ethanol and acetone before drying. The solvent was evaporated to yield a residue, which underwent purification through recrystallization in ethanol as outlined in Scheme 2.



Scheme 2. Synthesis of pyridine derivatives over the catalysis of $NiFe_2O_4$@SiO_2-AP-SO_3H

2.3 Selected NMR data

2-Amino-4,6-diphenylnicotinonitrile:^{1}H NMR (DMSO, 400 MHz): δ= 7.7 (m, 1H), 7.6 (m, 2H), 7.6 (m, 4H), 7.5 (m, 1H), 7.4 (m, 2H), 7.4(s, 1H), 6.5 (m, 2H) ppm.

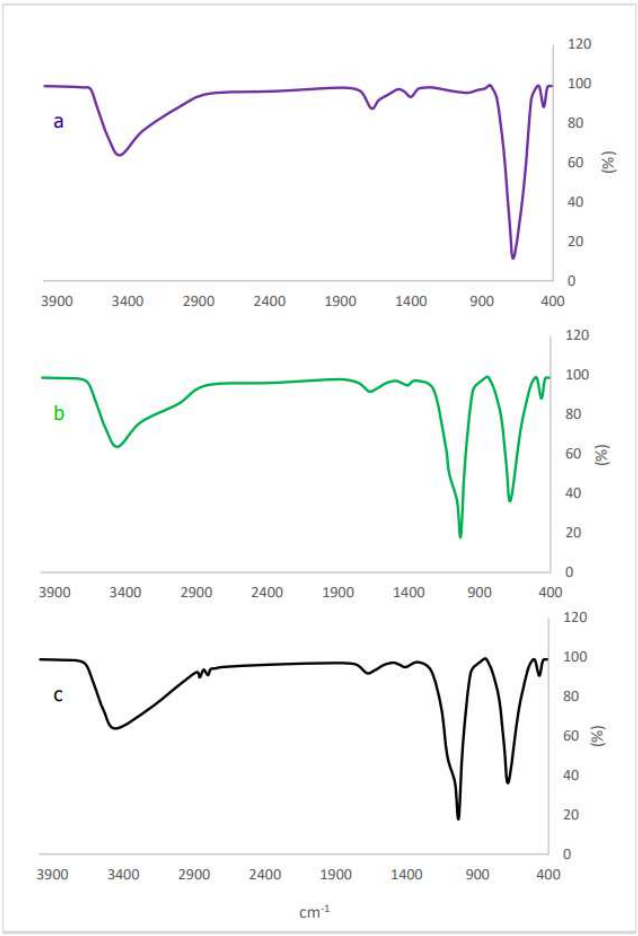
2-Amino-4-(3-nitrophenyl)-6-phenylnicotinonitrile:^{1}H NMR (DMSO, 400 MHz): δ= 8.0 (s, 1H), 7.7 (m, 1H), 7.7 (m, 1H), 7.6 (m, 7H), 6.5 (m, 2H) ppm.

2-Amino-4-(4-chlorophenyl)-6-phenylnicotinonitrile:^{1}H NMR (DMSO, 400 MHz): δ= 8.0 (s, 1H), 7.4 (m, 2H), 7.3 (m, 3H), 7.1 (m, 4H), 4.9 (s, 2H) ppm.

2-Amino-6-phenyl-4-(p-tolyl)nicotinonitrile:^{1}H NMR (DMSO, 400 MHz): δ= 7.9 (s, 1H), 7.6 (m, 4H), 7.5 (m, 3H), 7.3 (m, 2H), 4.7 (s, 2H), 1.2 (s, 3H) ppm.

3. Catalyst characterizations

FTIR spectra of $NiFe_2O_4$ (a), $NiFe_2O_4@SiO_2$ (b), $NiFe_2O_4@SiO_2$@n-Pr (c) $NiFe_2O_4@SiO_2$-AP (d) and $NiFe_2O_4@SiO_2$-AP-SO_3H (e) nanocatalyst is shown in Figure. 1. The FTIR spectrum of $NiFe_2O_4$ nanoparticles exhibits two bands at around 670 cm^{-1}, which are attributed to the stretching vibrations of the iron-oxygen bonds (Figure 1a). Furthermore, in Figure 1b, the presence of a stretching vibration band at 1033 cm^{-1} indicates the existence of Si-O bonds, providing evidence for the presence of SiO_2 on the surface of the $NiFe_2O_4$ nanoparticles. In Figure 1c, the C-H stretching vibration bands at 2809-3889 cm^{-1} confirm the presence of 3-chloropropyltriethoxysilane on the surface of $NiFe_2O_4@SiO_2$ NPs. In the spectrum of 3-aminopyridine ligand supported on $NiFe_2O_4@SiO_2$, the two broad bands at 3660 and 3490 cm^{-1} cans be ascribed to the N–H stretching vibration free NH_2 groups, respectively. In the spectrum of $NiFe_2O_4@SiO_2$-AP, the bands at 1572, and 1642 cm^{-1} are related to the C=N stretching of the ligand, which confirms the successful functionalization of $NiFe_2O_4@SiO_2$ with the ligand (**Figure 1d**). The incorporation of –SO_3H groups onto $NiFe_2O_4@SiO_2$-AP was confirmed by observing the absorption of OH stretching bands of the –SO_3H moiety at 2500–3500 cm^{-1} in the FTIR spectrum (**Figure 1e**) [30].


a
b
c
120
100
80
60
40
20
0
(%)
3900
3400
2900
2400
1900
1400
900
400
cm-1

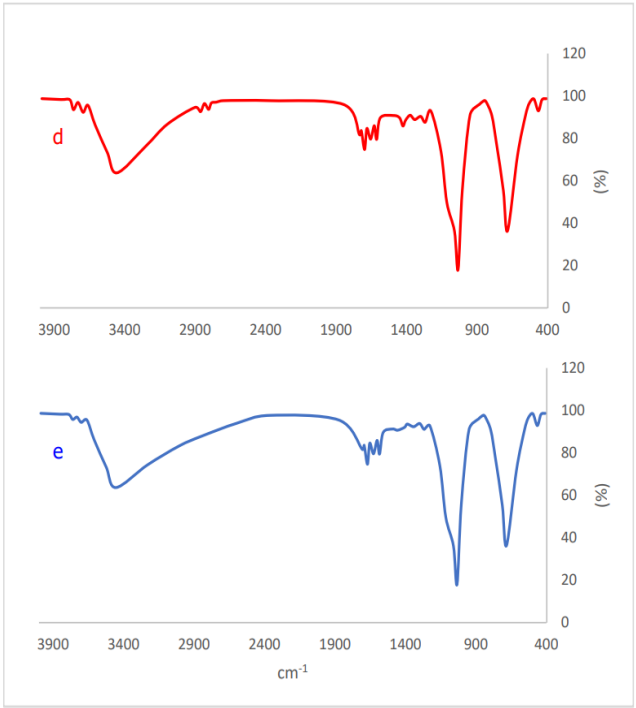

d
e
120
100
80
60
40
20
0
(%)
3900
3400
2900
2400
1900
1400
900
400
cm-1

Figure 1. Comparative study of FTIR spectra of a) $NiFe_2O_4$, b) $NiFe_2O_4@SiO_2$, c) $NiFe_2O_4@SiO_2$@n-Pr d) $NiFe_2O_4@SiO_2$-AP, and e) $NiFe_2O_4@SiO_2$-AP-SO_3H

To validate the crystalline phase of the synthesized $NiFe_2O_4$ and $NiFe_2O_4@SiO_2$-AP-SO_3H nanostructures, the indexed XRD patterns are presented in Figure 2. The $NiFe_2O_4$ spectrum reveals clear, distinct peaks corresponding to the (2 2 0), (3 1 1), (4 0 0), (4 2 2), (5 1 1), and (4 0 0) planes at 2θ angles of 30.3, 37.6, 43.4, 54.3, 57.8, and 64.4, respectively. From the XRD data, it can be deduced that the particles possess a face-centered cubic crystal structure.

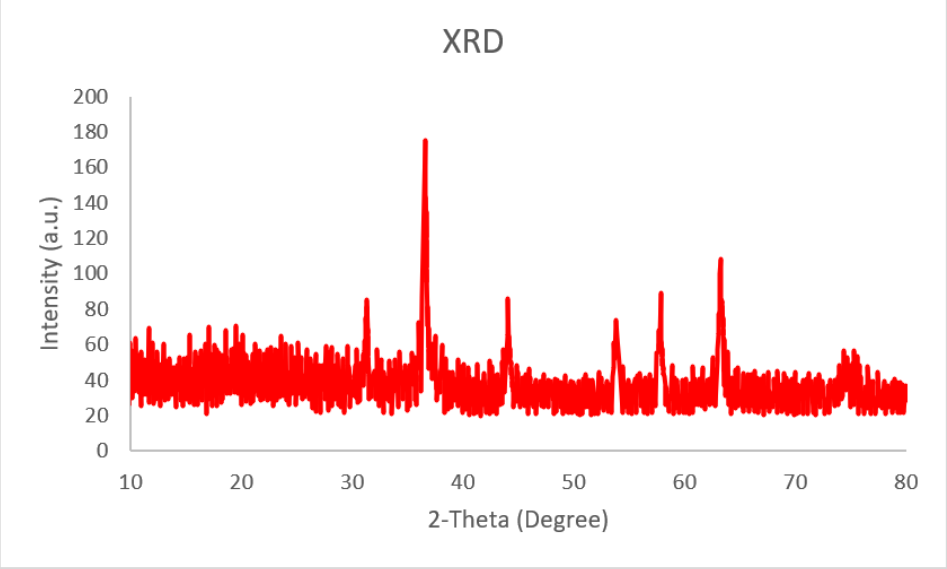


Figure 2. XRD spectrum of a) $NiFe_2O_4@SiO_2$-AP-SO_3H

The TGA was used to quantitatively determine the amount of ligand (AP-SO_3H) supported on the surface of $NiFe_2O_4$ magnetic nanoparticles. A minor weight loss of 6% below 250 °C was attributed to the removal of adsorbed solvents (Figure 3). In Figure 3, it is evident that $NiFe_2O_4@SiO_2$-AP-SO_3H exhibited a 25% weight loss between 250 and 700 °C, indicating the decomposition of the $NiFe_2O_4@SiO_2$-AP-SO_3H moieties. The TGA analysis results confirmed the successful support of AP-SO_3H on the surface of $NiFe_2O_4$.

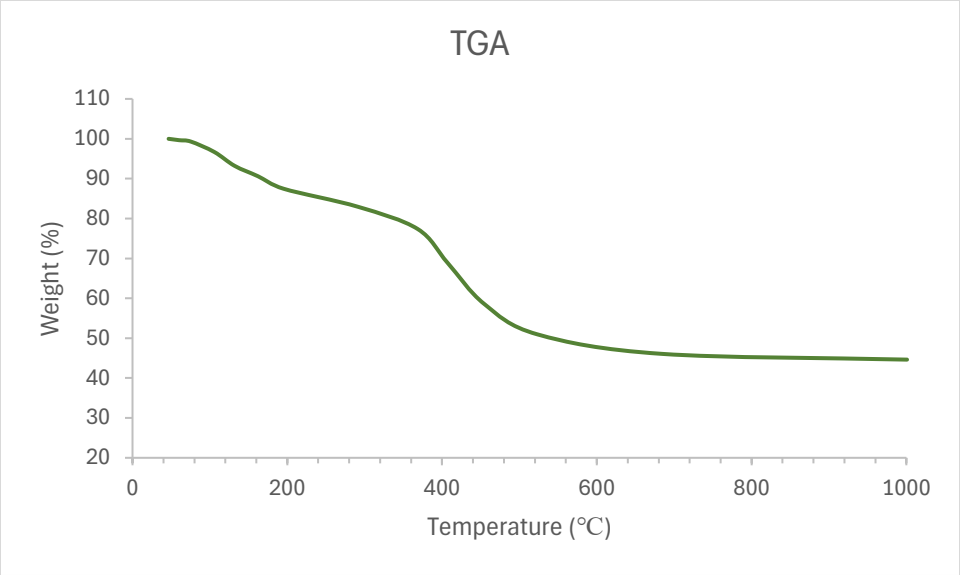


Figure 3. TGA curve of $NiFe_2O_4$@SiO_2-AP-SO_3H magnetic catalyst

The EDX image of the $NiFe_2O_4$@SiO_2-AP-SO_3H catalyst (Figure 4) reveals the presence of N, C, O, Si, Fe, S, and Ni elements. This indicates the absence of any additional impurities associated with the solvents and materials utilized in the catalyst synthesis process.

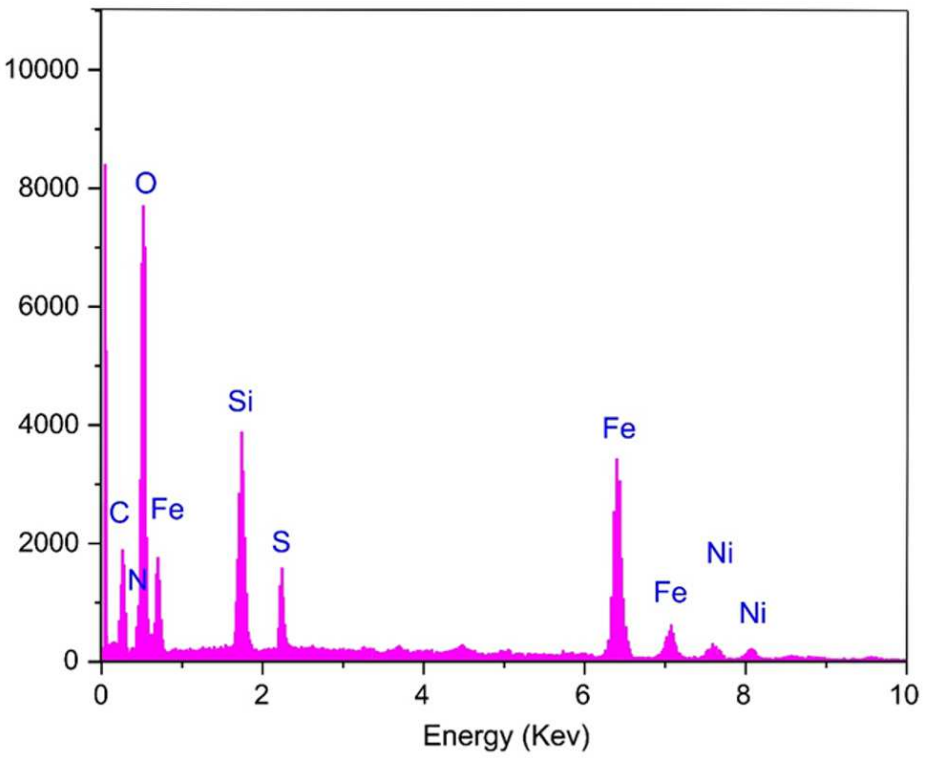


Figure 4. EDX images of $NiFe_2O_4$@SiO_2-AP-SO_3H.

Scanning Electron Microscopy (SEM) analysis was employed to thoroughly examine the structural attributes, including the shape, size, and morphological characteristics, of the synthesized catalyst. The SEM images provided in Figure 5 reveal that the nanoparticles exhibit a predominantly spherical configuration. Furthermore, these particles appear to be evenly distributed throughout the sample and display a consistent size range, indicating a uniform synthesis process.

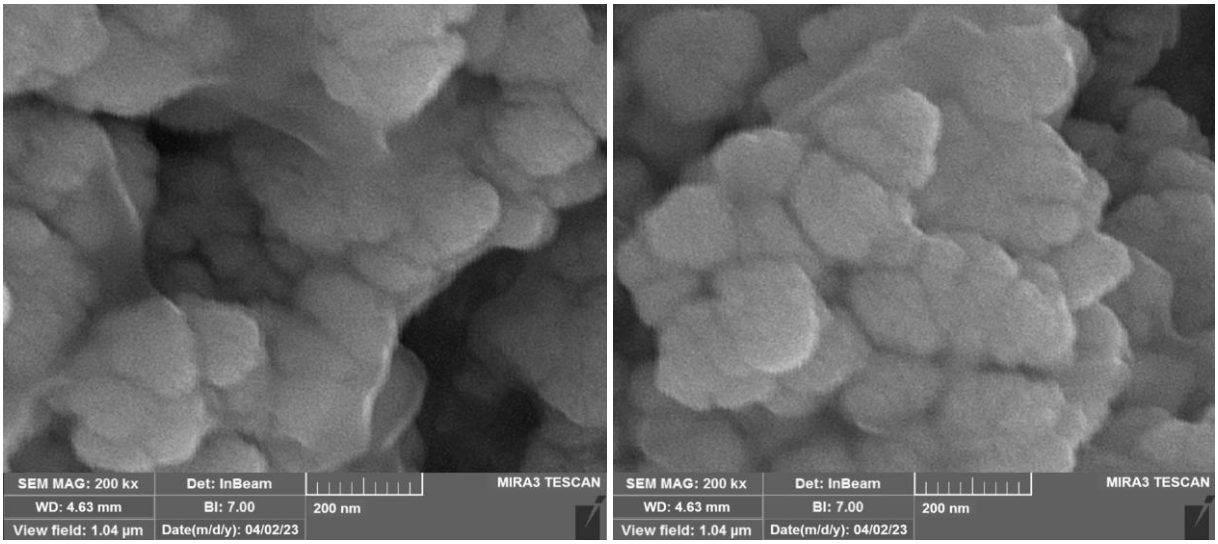


Figure 5. SEM images of $NiFe_2O_4$@SiO_2-AP-SO_3H.

The scanning electron microscopy images reveal that the nanocatalyst particles have a sphere-like structure and measure between 62 and 120 nanometers in size. These findings were corroborated by the data obtained from transmission electron microscopy images (Figure 6).

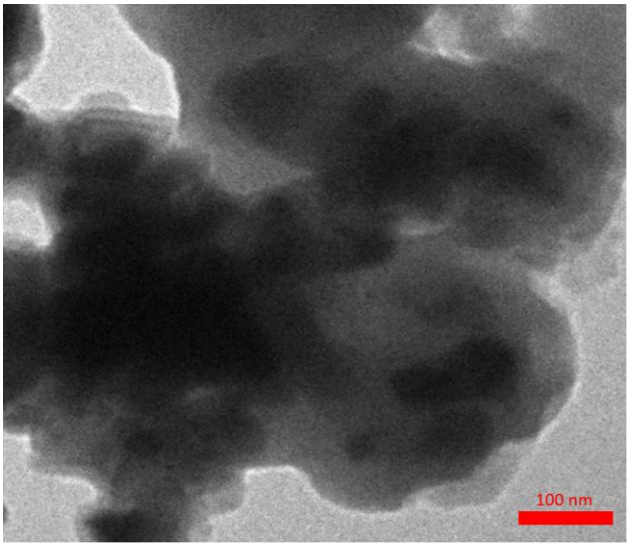


Figure 6 TEM images of $NiFe_2O_4$@SiO_2-AP-SO_3H.

The nanocatalyst's magnetic properties were examined through VSM analysis, with the findings presented in Figure 7. The saturation magnetization (Ms) value for the nanocatalyst is 36.51 emu/g, which is lower than that of the $NiFe_2O_4$ magnetic core. The functionalization of the $NiFe_2O_4$ NPs surface with AP-SO_3H has led to a reduction in saturation magnetization. Nevertheless, the synthesized nanocatalyst could be readily isolated from the reaction mixture using an external magnet.

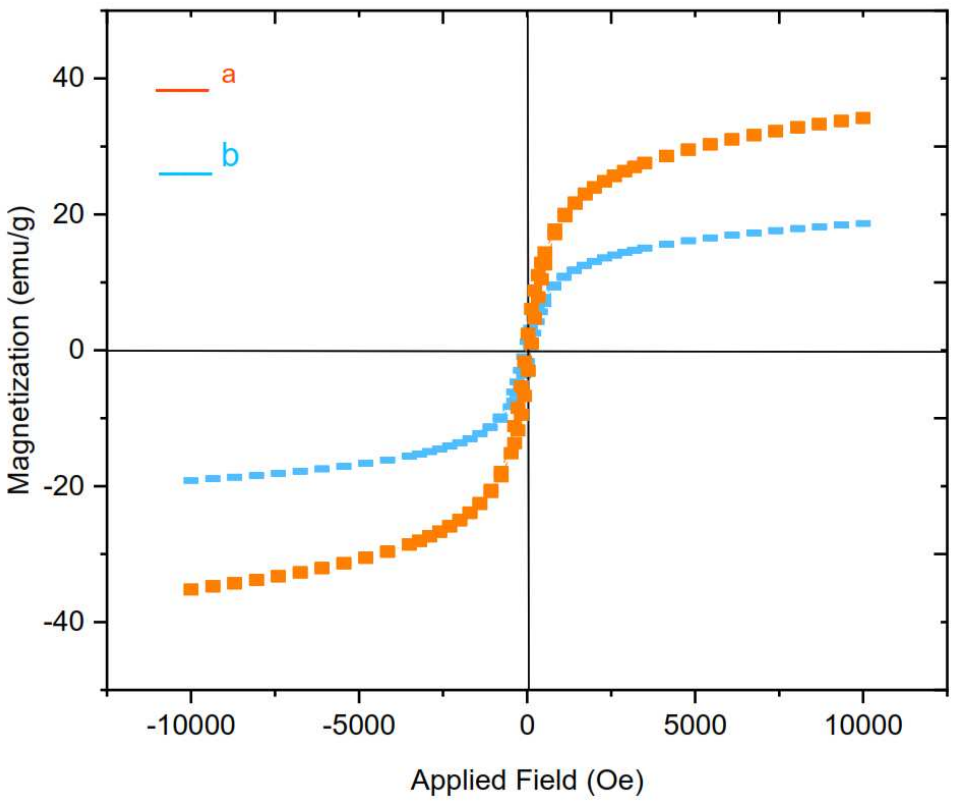


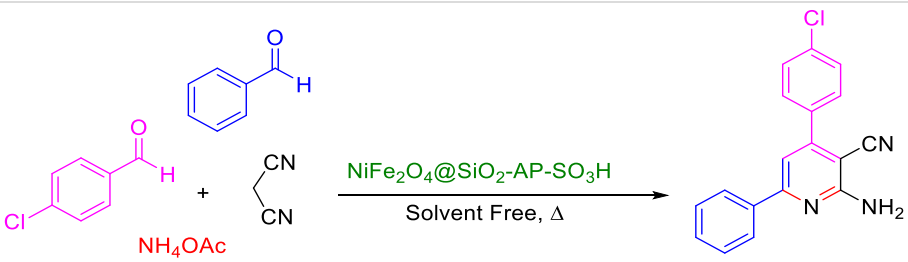
Figure 7 VSM curves of (a) $NiFe_2O_4$ (b) $NiFe_2O_4$@SiO_2-AP-SO_3H.

Catalytic studies:

In the second phase of the catalysis study, the direct synthesis of pyridines was explored using $NiFe_2O_4$@SiO_2-AP-SO_3H as the catalyst, with detailed results summarized in Table 1. The reaction involving 4-chlorobenzaldehyde, malononitrile, acetophenone, and ammonium acetate was first examined under solvent-free conditions at 80 °C without the catalyst. Under these conditions, only trace amounts of the desired product were obtained after more than 12 hours, alongside the formation of numerous side products. To enhance the reaction, varying amounts of $NiFe_2O_4$@SiO_2-AP-SO_3H were introduced. A clear increase in reaction rate and product yield was

observed as the catalyst loading increased from 10 mg to 25 mg, achieving an impressive 98% isolated yield of the target compound. Beyond this concentration, however, further increases in catalyst loading negatively affected the reaction's efficiency. Additional optimization efforts involved testing different solvents, including ethanol (EtOH), water (H_2O), dimethyl sulfoxide (DMSO), hexane, and dimethylformamide (DMF). All tested solvents led to a decline in performance when compared to the solvent-free approach. Consequently, a solvent-free system was determined to be optimal for further experimentation, with further adjustments focusing on reaction temperature. Through systematic testing, it was found that maintaining the reaction temperature at 80 °C yielded the best results, ensuring a maximum yield of 98%. Lower temperatures resulted in a marked decrease in reaction efficiency. Based on these findings, the optimal conditions for this transformation include using 20 mg of $NiFe_2O_4$@SiO_2-AP-SO_3H as a catalyst in a solvent-free medium at a temperature of 80 °C.

Table 3 Evaluation of reaction parameter on the synthesis of 2–amino–3–cyanopyridines over the catalysis of $NiFe_2O_4$@SiO_2-AP-SO_3H

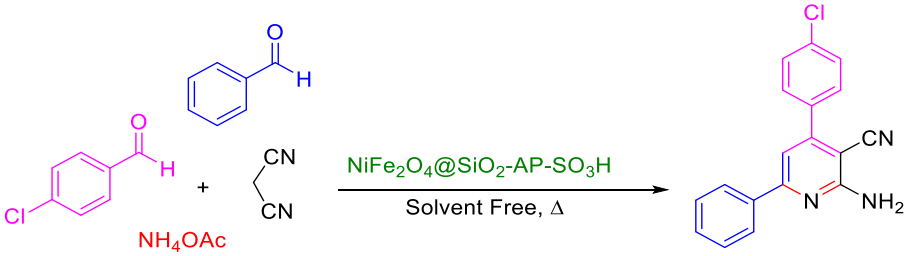


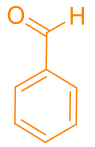
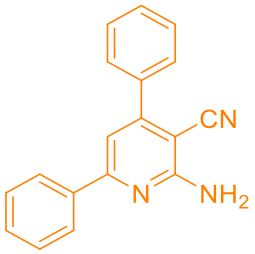
Entry	Catalyst(mg)	Solvent	Temperature(°C)	Time(min)	Yield (%)
1	-	Solvent Free	80	12 h	--
2	10	Solvent Free	80	1	40
3	15	Solvent Free	80	1	65
4	20	Solvent Free	80	1	98
5	25	Solvent Free	80	1	98
6	20	H_2O	Reflux	1	Trace
7	20	DMSO	100	1	83

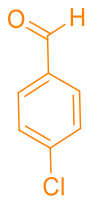
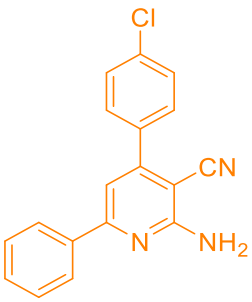
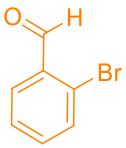
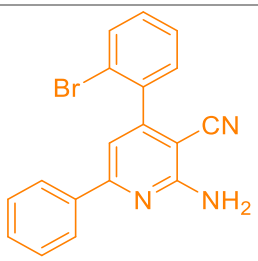
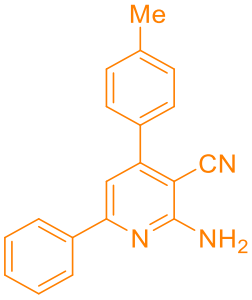
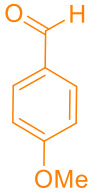
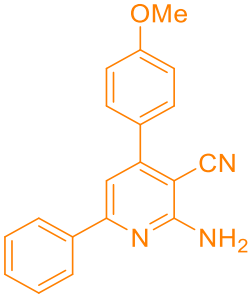
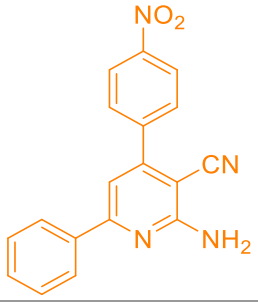
8	20	Hexane	Reflux	1	Trace
9	20	PEG-400	100	1	76
10	20	DMF	100	1	89
11	20	Ethanol	Reflux	1	51
12	20	Solvent Free	90	1	98
13	20	Solvent Free	50	1	60
14	20	Solvent Free	r.t	1	Trace

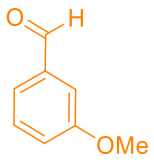
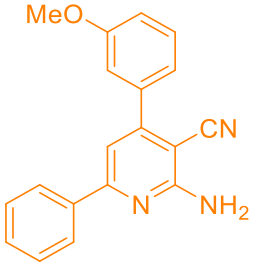
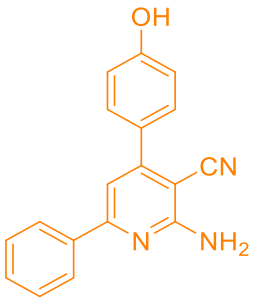
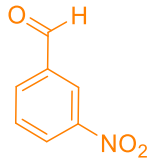
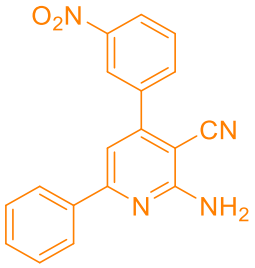
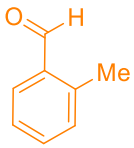
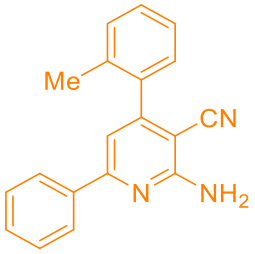
In the subsequent phase of synthesizing 2-amino-3-cyanopyridine derivatives, optimized reaction conditions were applied using a range of substituted aryl aldehydes for the specific durations listed in Table 2. Aldehydes containing both electron-withdrawing and electron-donating groups successfully produced the desired 2-amino-3-cyanopyridine compounds, yielding favorable results with efficiencies ranging from 81% to 98% within relatively short reaction times. Interestingly, aldehydes with electron-withdrawing substituents exhibited higher reactivity and achieved superior yields compared to those with electron-donating groups under identical experimental conditions.

Table 2 Synthesis of pyridine derivatives over the catalysis of $NiFe_2O_4@SiO_2$-AP-SO_3H



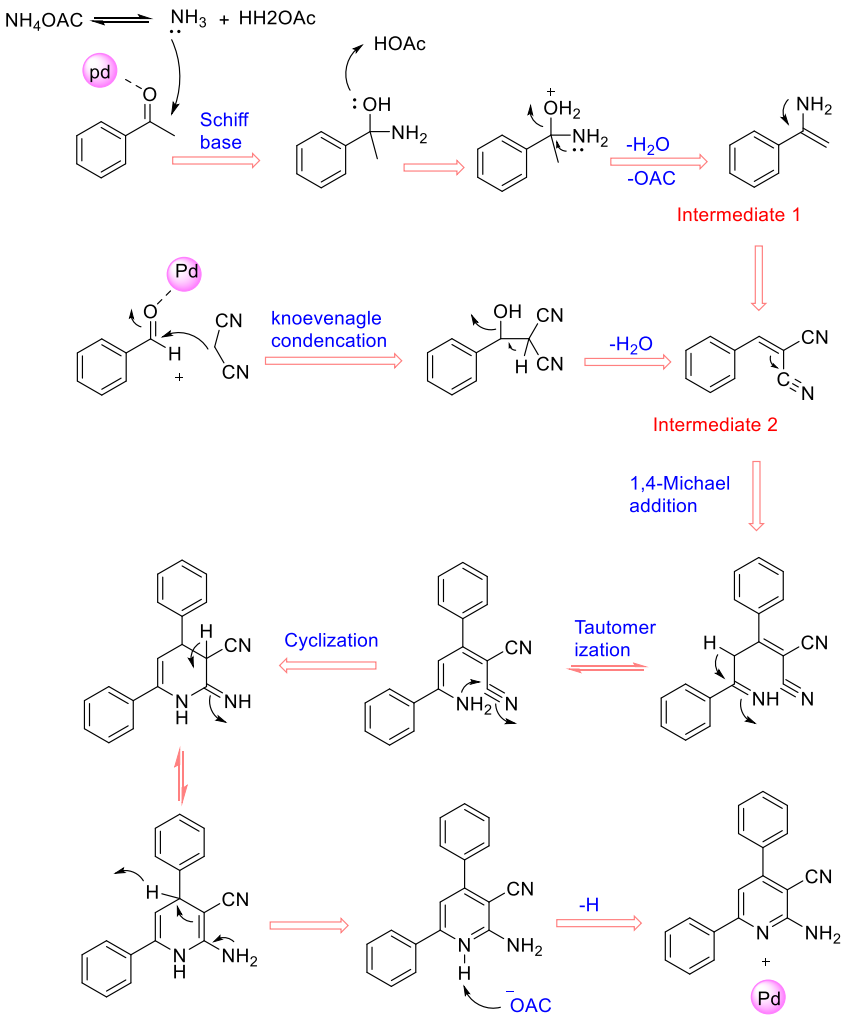
Entry	Aldehyde	Product	Time (h)	Yield (%)
1			1	96

2			1	98
3			45 min	81
4			45 min	90
5			30 min	96
6			1	91

7			40	94
8			30 min	94
9			1.5	94
10			20 min	89

Scheme 3 illustrates the synthesis mechanism for 2-amino-3-cyanopyridine derivatives using the $NiFe_2O_4$@SiO_2-AP-SO_3H catalyst. The process initiates with the catalyst facilitating the activation of the carbonyl group in an aldehyde, which then reacts with malononitrile to produce a Knoevenagel product. Simultaneously, ammonia undergoes nucleophilic addition to acetophenone, forming an imine intermediate. These intermediates subsequently engage in a 1,4-Michael addition, leading to their condensation and resulting in a new intermediate. This intermediate undergoes a Thorpe-Ziegler-type cyclization, producing a six-membered ring structure containing nitrogen. Within this ring, both the exocyclic and endocyclic anomeric

nitrogen atoms align effectively to resonate with the C–C double bonds. This resonance facilitates hydride ion removal through a cooperative geminal-vinylogous anomeric-based oxidation mechanism, corroborated by conducting the reaction under a nitrogen atmosphere. The transformation is primarily driven by the enhanced stability of the aromatic pyridine product formed, as depicted in Scheme 3.



Scheme 3. Plausible mechanism for the synthesis of 2-amino-3-cyanopyridines over the catalysis of $NiFe_2O_4@SiO_2$-AP-SO_3H

Hot filtration

Under optimal reaction conditions hot filtration experiment was conducted to assess the heterogeneous nature of the $NiFe_2O_4$@SiO_2-AP-SO_3H catalyst. In the absence of the catalyst, the maximum yield of 2-amino-3-cyanopyridines was only 3% after 1 hour, revealing the necessity of an acid catalyst for the progression of the reaction. Conversely, the introduction of the $NiFe_2O_4$@SiO_2-AP-SO_3H catalyst led to a remarkable increase in the 2-amino-3-cyanopyridines yield, reaching 96% within 1 hour. This clearly demonstrates the catalytic prowess in enhancing the reaction rate.

4. Catalyst recyclability

In another examination to assess the recyclability of the magnetic catalyst, we conducted a test using benzaldehyde as a model reaction with 0.02 g of $NiFe_2O_4$@SiO_2-AP-SO_3H. After the reaction, the catalyst was retrieved from the mixture using a magnet, followed by multiple washings with H_2O and EtOH. Remarkably, the catalyst maintained its activity over four consecutive runs without any significant loss (see Figure 8).

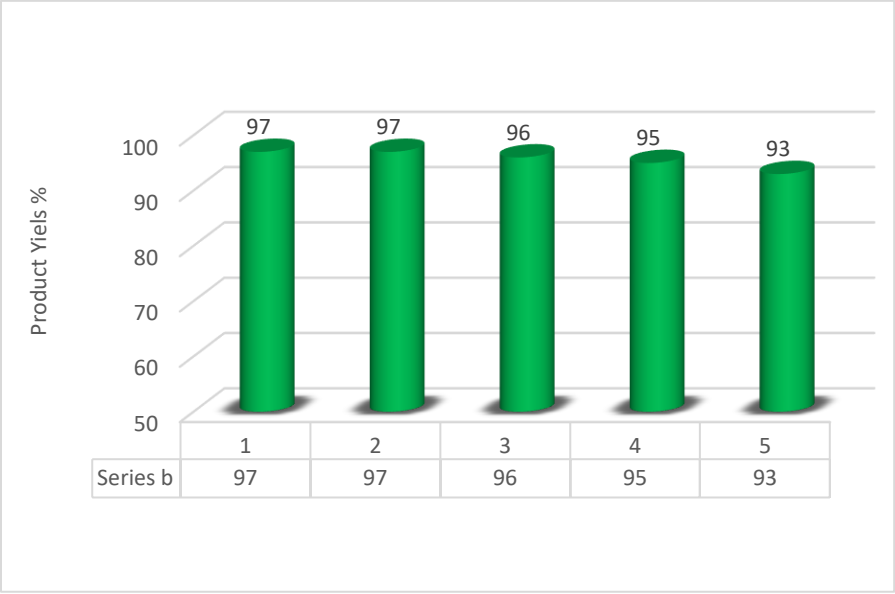


Figure 8. Recyclability of $NiFe_2O_4$@SiO_2-AP-SO_3H in the synthesis of synthesis of 2-amino-3-cyanopyridines

5. Conclusion

In this work, we have developed a reliable and straightforward method for producing $NiFe_2O_4$@SiO_2-AP-SO_3H as a magnetically retrievable nanocatalyst, characterized through diverse techniques. The developed catalyst, $NiFe_2O_4$@SiO_2-AP-SO_3H, underwent characterization through SEM, EDS, VSM, TGA, XRD, TEM, and FT-IR analyses. The $NiFe_2O_4$@SiO_2-AP-SO_3H materials exhibited excellent efficiency in synthesis of pyridine derivatives. The method offers several advantages, including a straightforward work-up procedure, the use of nontoxic solvents, high yield, short reaction time, good tolerance of various functional groups, and the ability to recycle and reuse the catalyst using an external magnet for up to 4 runs, with only a notable decrease in product yields.

Data availability

All data generated or analyzed during this study are included in this published article [and its supplementary information files].

Acknowledgment

The authors extend their appreciation to Faculty of Allied Medical Sciences, Hourani Center for Applied Scientific Research, Al-Ahliyya Amman University, Amman, Jordan.

Role of the funding source

The authors declare that they have no known competing financial interests or personal relationships that could have appeared to influence the work reported in this paper.

References

1. Hasan, K., Joseph, R. G., Patole, S. P. & Al-Qawasmeh, R. A. Development of magnetic Fe3O4-chitosan immobilized Cu(II) Schiff base catalyst: An efficient and reusable catalyst for microwave assisted one-pot synthesis of propargylamines via A3 coupling. *Catal. Commun.* **174**, 106588 (2023).

2. Anizadeh, M. R., Torabi, M., Zolfigol, M. A. & Yarie, M. Catalytic application Fe3O4@SiO2@(CH2)3-urea-dithiocarbamic acid for the synthesis of triazole-linked pyridone derivatives. *J. Mol. Struct.* **1277**, 134885 (2023).

3. Ismail, H. A. & Abed, R. R. Synthesis, characterization, and biological activity assessment of new metal complexes of Schiff bases produced from benzoin. *Al-Kitab J. Pure Sci.* **7**, 27–41 (2023).

4. Zhang, H., Zhang, L.-L., Tan, X., Li, H. & Yang, S. Catalytic high-yield biodiesel production from fatty acids and non-food oils over a magnetically separable acid nanosphere. *Ind. Crops Prod.* **173**, 114126 (2021).

5. Rivero, M. *et al.* Toxicity and biodegradation of zinc ferrite nanoparticles in Xenopus laevis. *J. Nanoparticle Res.* **21**, 1–30 (2019).

6. Mirbagheri, R. & Elhamifar, D. Magnetic ethyl-based organosilica supported Schiff-base/indium: A very efficient and highly durable nanocatalyst. *J. Alloys Compd.* **790**, 783–791 (2019).

7. Hadrup, N. *et al.* Pulmonary toxicity of Fe2O3, ZnFe2O4, NiFe2O4 and NiZnFe4O8 nanomaterials: Inflammation and DNA strand breaks. *Environ. Toxicol. Pharmacol.* **74**, 103303 (2020).

8. Priyadarshini, M., Ahmad, A. & Ghangrekar, M. M. Efficient upcycling of iron scrap and waste polyethylene terephthalate plastic into Fe3O4@C incorporated MIL-53(Fe) as a novel electro-Fenton catalyst for the degradation of salicylic acid. *Environ. Pollut.* **322**, 121242 (2023).

9. Fatimah, I. *et al.* One-pot synthesis of Fe3O4/NiFe2O4 nanocomposite from iron rust waste as reusable catalyst for methyl violet oxidation. *Case Stud. Chem. Environ. Eng.* **8**, 100369 (2023).

10. Vahid, N. F., Marvi, M. R., Naimi-Jamal, M. R., Naghib, S. M. & Ghaffarinejad, A. X-Fe2O4-buckypaper-chitosan nanocomposites for nonenzymatic electrochemical glucose biosensing. *Anal. Bioanal. Electrochem.* **11**, 930–942 (2019).

11. Lalhmangaihzuala, S. *et al.* Orange peel ash coated Fe3O4 nanoparticles as a magnetically retrievable catalyst for glycolysis and methanolysis of PET

waste. *Adv. Powder Technol.* **34**, 104076 (2023).

12. Gorgizadeh, M. *et al.* Sonodynamic cancer therapy by a nickel ferrite/carbon nanocomposite on melanoma tumor: In vitro and in vivo studies. *Photodiagnosis Photodyn. Ther.* **27**, 27–33 (2019).

13. Hadrup, N. *et al.* Pulmonary toxicity of Fe2O3, ZnFe2O4, NiFe2O4 and NiZnFe4O8 nanomaterials: inflammation and DNA strand breaks. *Environ. Toxicol. Pharmacol.* **74**, 103303 (2019).

14. Satyanarayana, L., Reddy, K. M. & Manorama, S. V. Nanosized spinel NiFe2O4: A novel material for the detection of liquefied petroleum gas in air. *Mater. Chem. Phys.* **82**, 21–26 (2003).

15. Zhang, S. *et al.* Study on the construction of char-supported NiFe-NiFe2O4 catalyst and its catalytic cracking mechanism of biomass tar under relative low temperature. *Fuel* **346**, 128412 (2023).

16. Abed M. Al-Jewaree, H. & Adil M.Ali, O. An experimentally investigate the effect of physical properties on the production of lubricating materials from crude oils. *Al-Kitab J. Pure Sci.* **3**, 30–47 (2022).

17. Malysheva, S. *et al.* Phosphine chalcogenides and their derivatives from red phosphorus and functionalized pyridines, imidazoles, pyrazoles and their antimicrobial and cytostatic activity. *Bioorg. Chem.* **132**, 106363 (2023).

18. Afsar, J. *et al.* Synthesis and application of melamine-based nano catalyst with phosphonic acid tags in the synthesis of (3′-indolyl)pyrazolo[3,4-b]pyridines via vinylogous anomeric based oxidation. *Mol. Catal.* **482**, (2020).

19. Sandaroos, R., Maleki, B., Naderi, S. & Peiman, S. Efficient synthesis of sulfones and sulfoxides from sulfides by cobalt-based Schiff complex supported on nanocellulose as catalyst and Oxone as the terminal oxidant. *Inorg. Chem. Commun.* **148**, 110294 (2023).

20. Utsugi, T. *et al.* Antitumor activity of a novel quinoline derivative, TAS-103, with inhibitory effects on topoisomerases I and II. *Jpn. J. Cancer Res.* **88**, 992–1002 (1997).

21. Sebris, A. & Turks, M. Recent investigations and applications of azidoazomethine-tetrazole tautomeric equilibrium (microreview). *Chem. Heterocycl. Compd.* **55**, 1041–1043 (2019).

22. Zong, Y. *et al.* Activation of peroxymonosulfate by a magnetic Co doped

NiFe2O4 catalyst for efficient Bisphenol A degradation in water. *J. Taiwan Inst. Chem. Eng.* **147**, 104930 (2023).

23. Benaboud, A. *et al.* Fe2O4/ZnO-nanowires synthesis by dip-coating for Orange II-dye photodegradation. *Optik (Stuttg).* **144**, 397–405 (2017).

24. Yang, J. *et al.* Microwave-assisted one-step production of biodiesel from waste cooking oil by magnetic bifunctional SrO–ZnO/MOF catalyst. *J. Clean. Prod.* **395**, 136182 (2023).

25. Sánchez-Férez, F., Calvet, T., Font-Bardia, M. & Pons, J. The Formation of a Unique 2D Isonicotinate Polymer Driven by Cu(II) Aerobic Oxidation. *Materials* vol. 16 (2023).

26. Kurahashi, M. & Sun, X. Observation of a Half-Metallic Interface State for Pyridine-Adsorbed H/Fe3O4(100). *J. Phys. Chem. Lett.* 8489–8494 (2021) doi:10.1021/acs.jpclett.1c02391.

27. Balalaie, S., Derakhshan-Panah, F., Zolfigol, M. A. & Rominger, F. A Convenient Method for the Synthesis of Imidazo[1,2- a]pyridines with a New Approach. *Synlett* **29**, 89–93 (2018).

28. Zhang, X., Bai, F., Li, M., Ru, H. & Wang, L. NiFe2O4@SiO2@PrNH2–DPA–CeCl3: a cerium-based magnetic nano dual-acid catalyst with high efficacy and recyclability for domino sequential synthesis of lactam ring-fused 1,5-benzodiazepines. *Catal. Sci. Technol.* **13**, 3987–3999 (2023).

29. Hajiarab, R., Mohammad Shafiee, M. R. & Ghashang, M. Access to a Library of 3-(9-Methyl-9H-Carbazol-3-yl)-2-Arylthiazolidin-4-One Derivatives Using NiFe2O4@SiO2 Grafted Alkyl Sulfonic Acid as an Efficient Catalyst. *Polycycl. Aromat. Compd.* **43**, 2032–2043 (2023).

30. Kalantari, F. *et al.* SO3H-Functionalized Epoxy-Immobilized Fe3O4 Core–Shell Magnetic Nanoparticles as an Efficient, Reusable, and Eco-Friendly Catalyst for the Sustainable and Green Synthesis of Pyran and Pyrrolidinone Derivatives. *ACS Omega* (2023) doi:10.1021/acsomega.3c01068.

Supplementary Files

This is a list of supplementary files associated with this preprint. Click to download.

- suportingfinal.docx